

# Non-reductive Homolytic Scission of Endoperoxide Bond for Activation of Artemisinin: *The Bi-radical Perspectives*

Shikha Sharma<sup>a</sup>, Md. Ehesan Ali\*<sup>a</sup>

*Institute of Nano Science and Technology, Sector-81, Mohali, Punjab, 140306*

*India*

\*Email: [ehesan.ali@inst.ac.in](mailto:ehesan.ali@inst.ac.in)

## Abstract

Artemisinin is the most famous antimalarial drug against malaria caused by *Plasmodium falciparum*. Despite its tremendous success and popularity in malaria therapeutics, the molecular mechanism of artemisinin's activity is still elusive. The activation of artemisinin, i.e., cleavage of the endoperoxide bond at the infected cell that generates radical intermediates and the subsequent chemical rearrangements plays a key role in the antimalarial activities. In this work, applying state-of-the-art computational techniques based on the spin constraint density functional theory (CDFT) along with *ab initio* thermodynamics, we have investigated various key steps of the molecular mechanism of artemisinin. The well-accepted artemisinin activation process is the reductive heterolytic scission of the endo-peroxide bond which is followed by subsequent chemical reactions that propagate via mono-radical intermediates. Here adopting the CDFT we have investigated the possible alternative 'biradical' intermediates and their mechanistic pathways for the subsequent chemical reactions. The change in Gibbs free energy associated with the activation of artemisinin through homolytic-scissoring (biradical) intermediate is quite competitive and favorable compared to the reductive heterolytic-scissoring (monoradical) process. This clearly indicates the alternative possibilities for the biradical activation process. The reported experimental EPR signals for the biradicals especially for similar anti-malarial drugs like G3-factor support our observations.

## 1. Introduction

Malaria is one of the most widespread parasitic diseases caused by protozoan parasites of the class of *Plasmodium*. It is the leading cause of death in several tropical sub-Saharan countries, where young children and pregnant women are most affected.<sup>1,2</sup> The disease not only costs human life but has a huge impact on socio-economic issues across the globe.<sup>3</sup> According to the

World health organization, 3.2 billion people (half the world's population) live in areas at risk of malaria transmission in 106 countries and territories. As per the 2020 WHO report, malaria caused an estimated 229 million clinical incidents and 405,000 related deaths. Most of these malaria cases were observed in African Regions (215 million or 94%) followed by the South-East Asia region with 3.4% of the cases.<sup>4</sup>

*Plasmodium falciparum* is the deadliest species of plasmodium that causes malaria in humans and transmitted through the *Anopheles* mosquito.<sup>5</sup> For its survival, *Plasmodium falciparum* digests the globin protein of the red blood cells and releases free heme inside the food vacuole of the parasite which is potentially toxic to the parasite.<sup>6</sup> To avoid this toxicity, the parasite converts it into hemozoin which undergoes dimerization to form beta-hemozoin and then undergoes the bio-crystallization process to form hemozoin, which is known as malaria pigment.<sup>7-9</sup>

The traditional quinoline based antimalarial drugs such as chloroquine and quinine function by inhibiting the beta-hemozoin formation due to reversible binding of the drug at the axial position of the free-heme.<sup>10-14</sup> The toxicity of free heme is responsible for the death of the parasite. However, the most successful drug is the endoperoxide based artemisinin, which targets the food vacuole of the parasites directly. The activation of artemisinin i.e., cleavage of the endoperoxide bonds and generation of the radical species could occur either by homolytic or heterolytic scission of the endoperoxide O-O bonds.<sup>15-18</sup> The widely discussed mechanism is the heterolytic one, in which one electron reduction process is involved. The source of the  $1e^-$  has been discussed as the oxidation process of Ferro-protoporphyrin-IX (Fe(II)PPIX) to Ferri-protoporphyrin-IX (Fe(III)PPIX) during the digestion of hemoglobin by the parasites in the infected red-blood cell (RBC).<sup>19-20</sup>

A large number of literatures are available for the reductive cleavage of endoperoxide bonds based on experimental studies and confirmed by various spectroscopic properties i.e., FTIR spectra, Raman and Infrared studies, NMR and from EPR spectroscopy.<sup>21-24</sup> These studies showed that the cleavage of endoperoxide bonds is induced by heme/Fe (II) ions to produce oxygen-centered radicals. These radicals subsequently rearrange into carbon centered radical species either by 1,5-H shift or by homolytic cleavage of C-C bond.<sup>25-27</sup> It was further validated by EPR spectra that the spin trapped free radical signal occurs only when artemisinin is incubated in the presence of iron. This reductive mono-radical mechanism has largely been discussed in the literature and adopted in various theoretical studies as well.<sup>28-34</sup>

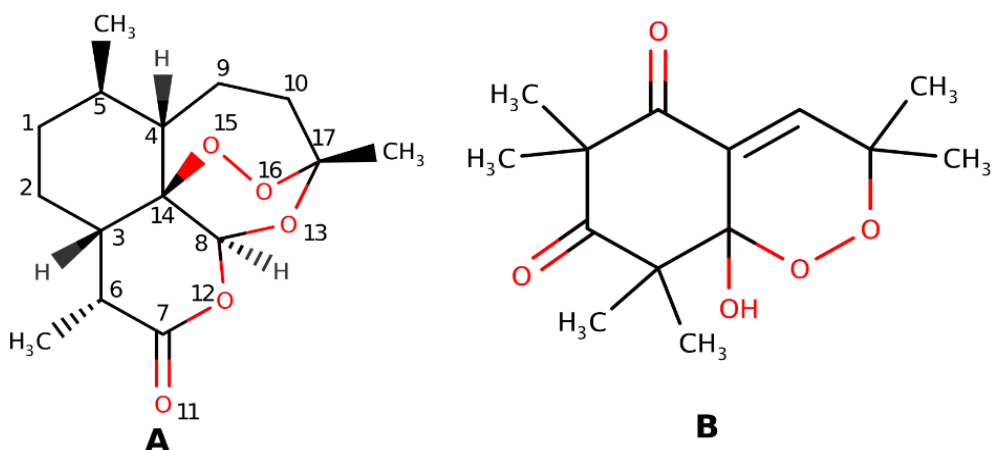


**Fig.1** Structures of popular antimalarial drugs against *Plasmodium falciparum* (A) Artemisinin and (B) G3-factor. In the newly developed endoperoxide-containing drug i.e., G3-factor it is already identified as the biradical intermediates by EPR spectra.

The other possibility of artemisinin activation i.e., homolytic cleavage of the endoperoxide bond that has also been discussed in endoperoxide based G3-factor antimalarial drugs (structures shown in Fig.1B).<sup>35</sup> However, only few literatures are available for homolytic cleavage of the endoperoxide bonds with biradical intermediate.<sup>36-39</sup> The biradical intermediates was detected in EPR spectroscopy and also indicated in other theoretical studies as well.<sup>40</sup>

In this work, we have investigated and compared the activation of artemisinin through both the possibilities and the subsequent chemical rearrangements of the activated bi-radical species by applying state-of-the-art spin-constraint density functional theory (CDFT)<sup>41-43</sup>, along with the standard DFT<sup>44</sup> method. The recent advancement of the CDFT methodology has enabled one to investigate the bi-radical intermediates confining the spin-centers at the selected sites that is not possible to achieve in the standard DFT based methodologies.

## 2. Computational Details

To investigate the activation of artemisinin and its subsequent reaction intermediates, the molecular geometries and electronic structures for all the species were computed using the B3LYP/6-311G(d,p)<sup>45</sup> methodology after a rigorous benchmarking of DFT methodologies and basis sets (See SI). The quantum chemical code *Orca 4.0*<sup>46</sup> was used for the DFT calculations. All the calculations were performed within the unrestricted Kohn-Sham formalism treating the radical species as open-shell molecules within the DFT framework. However, in the standard DFT methods even with hybrid functional over delocalization of the electron or spin-density occurs over an extended region. This over-delocalization in the standard DFT limits the study

of resulting various intermediate radical species upon localizing the spin-densities in the different atomic sites. To tackle this scenario, a recently developed spin-constraint density functional theory (CDFT) is also applied. The latter method has been implemented in *Nwchem* 6.6 quantum chemistry code.<sup>47</sup> This constraint DFT approach prevents any spurious spin delocalization applying spatial constraints on the spin densities during the self-consistent optimization of the densities. The Lowdin spin population was used in order to apply the constraint. The *ab initio* thermodynamics properties such as the reaction free energy i.e.,  $\Delta G$ ,<sup>48-50</sup> were computed by applying standard DFT as well spin-constraint CDFT methodologies. The solvent effect on the energies for the activation of the artemisinin has also been studied, by using the COSMO<sup>51,52</sup> approach in different solvents medium at B3LYP/6-311G (d,p) level.

### 3. Results and Discussion

#### 3.1. Activation of artemisinin

For the activation of artemisinin there are two possibilities, one is heterolytic scission and the other one is homolytic cleavage of O-O bond. In this work we have investigated the heterolytic as well homolytic cleavage applying the standard DFT (B3LYP) and constraint spin-density functional theory (CDFT) calculations. The computed corresponding spin-densities are plotted in Fig. 2. It is quite evident that the spin density obtained from the DFT calculations for the mono-radical description is quite unusual as it has been distributed among the two O-atoms (O<sub>15</sub> & O<sub>16</sub>) symmetrically with 0.49 and 0.42  $\mu_B$  magnetic moments. This is the artifact of the DFT due to the self-interaction error (SIE). To obtain the appropriate description of the mono-radical species the spin-constraint DFT, that confine the unpaired electrons within its designated site during the self-consistent optimization of the wavefunction. Thus, CDFT is a more logical and pragmatic approach to handle the SIE. The comparison of the spin-density plot for activated mono-radical in Fig. 2a & 2b clearly indicates the CDFT recovers the asymmetric nature of the spin-density with 1.0 on O<sub>16</sub> and 0.16  $\mu_B$  on O<sub>15</sub>. For activated diradical with localized spins on the two O-atoms is similar to mono-radical counterpart but with two electrons are localized symmetrically on the two oxygen atoms. However, DFT produces slightly more delocalized spin-moments on the oxygen atoms with 0.79 and 0.76  $\mu_B$ , and the spilled/delocalized spin-moments could be visualized in the neighboring atoms (Fig. 2c). Employing CDFT methods it recovers the spurious spin-moments and localizes 0.88 and 0.85  $\mu_B$  on the O-atoms.

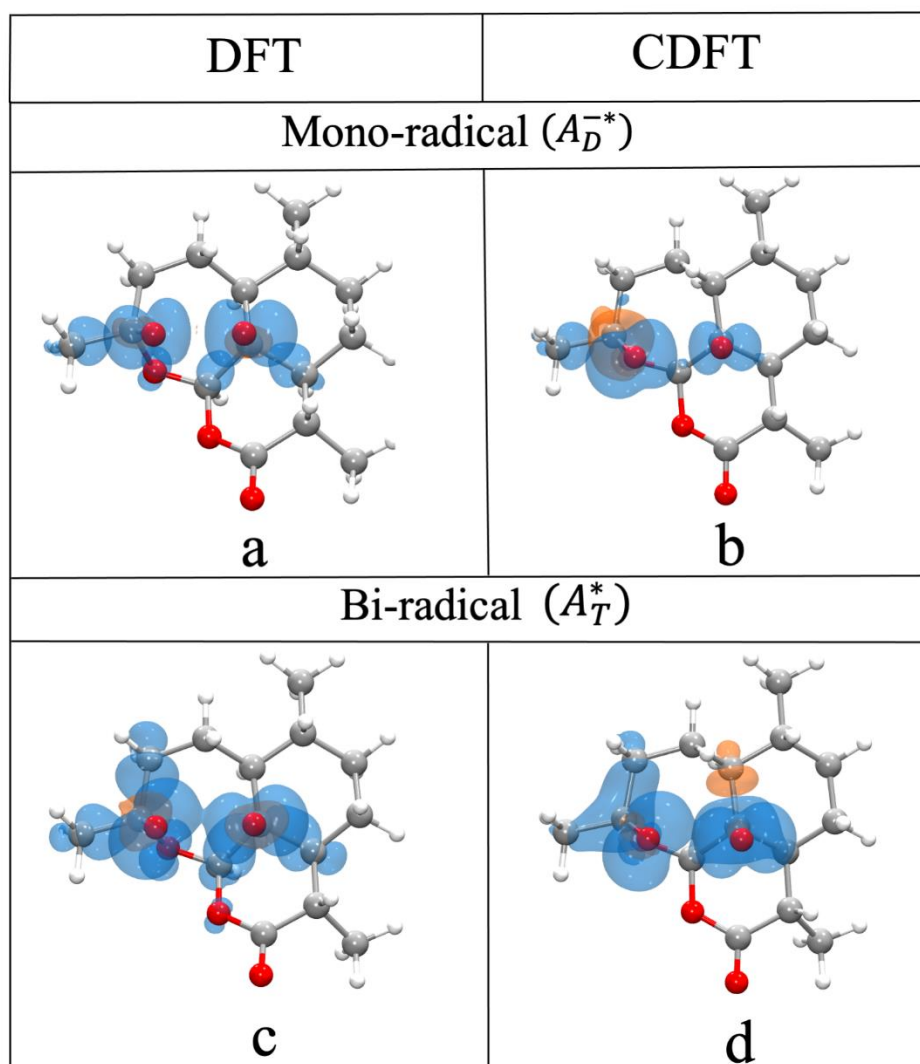
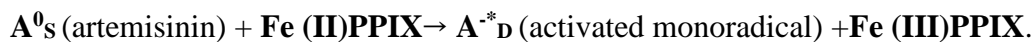


**Fig.2** The spin density distribution obtained for the activation of artemisinin through heterolytic and homolytic cleavage process adopting DFT (UB3LYP/6-311G\*\*) and CDFT (UB3LYP/6-311G\*\*) method. The  $\alpha$  and  $\beta$  spin-densities are now shown in blue and orange colours respectively with isovalue of  $0.002 \mu_B/\text{\AA}^3$ . The detailed spin density for the individual atoms could be found in Table S3.)

The  $\Delta G$  for one electron reductive cleavage (i.e., heterolytic scission) is calculated by various computational methods that explored the possible mechanism.<sup>30,31</sup> A few of them have reported that without any activation barrier the peroxide bond can break or it can go for a thermodynamically favorable reaction.<sup>28,31</sup> Following the procedures mentioned in the previous reports, we have also verified the (erroneous) exothermic process for the activation of artemisinin by heterolytic cleavage with  $\Delta G$  of  $-51.40$  kcal/mol. However, the  $\Delta G$  computed in those earlier reports are doubtful as the total number of electrons between the reactants and products were not conserved. The accurate calculation of the thermodynamic parameters of a chemical reaction must obey the isoelectronicity between the reactants and products.<sup>53-56</sup>

Adopting the isoelectronic behavior, we have computed the free energy of activation (i.e.,  $\Delta G$ ) for both the activation pathways. To compute the  $\Delta G$  with the isoelectronic method for reductive heterolytic cleavage, we have considered the following chemical reaction



The reason behind incorporating the **Fe(II)PPIX/Fe(III)PPIX** redox couple in the one electron activation process. The ferro-protoporphyrin **Fe(II)PPIX** is released upon parasite hemoglobin digestion and Fe (II) is oxidized to Fe (III) in the detoxification process by releasing an electron which has been hypothesized as source of the electron for the one electron transfer activation of artemisinin.<sup>16</sup> Free energies associated with the monoradical activation of artemisinin in a single-molecule environment along with different solvent environments are also given in SI. However, for the homolytic cleavage no additional redox couple is necessary as there is no change in the total number of electrons. Adopting the isoelectronic behavior, we obtained 81.67 (in gas phase) and 23.64 (in water) and 26.54 (in DMSO) kcal/mol  $\Delta G$  for the heterolytic cleavage of endoperoxide bond instead of -51.40 kcal/mol.

The bi-radical free energies are investigated upon vertical singlet to triplet excitations ( $A^0_s \rightarrow A^V_T$ ) followed by the adiabatic triplet state search that spontaneously undergoes the homolytic cleavage of the O-O bond and forms the *bi-radical* intermediates. The free energy of activations is obtained from the free energy difference of the adiabatic singlet (i.e.,  $A^0_s$  ground state) and adiabatic triplet states ( $A^*_T$ ). It is further observed that the adiabatic state of the activated artemisinin ( $A^*_T$ ) resides 24.01 kcal/mol above the neutral singlet-state. This is considerably lower than the free energy of activation for the activated mono-radical (81.67 kcal/mol) in the single-molecule environment.

In solvent environments the computed free energies become quite competitive in fact lower than the mono-radical pathways with  $\Delta G$  values of 21.77 (in water) and 21.82 (in DMSO) kcal/mol. Furthermore, it is also observed that the activated bi-radical triplet state is more stable compared to the singlet-biradicals by 1.96 Kcal/mol. The computed free energy of activation for bi-radical intermediates in single-molecule environments is 24.01 kcal/mol compared to 80.67 kcal/mol for monoradical intermediates. This is quite a large difference, however in presence of solvent medium the energies become comparable. In fact, the comparison of  $\Delta G$  in the solvent medium indicates the bi-radical mechanism is more plausible compared with mono-radicals in the physiological conditions mimicked by water and DMSO.

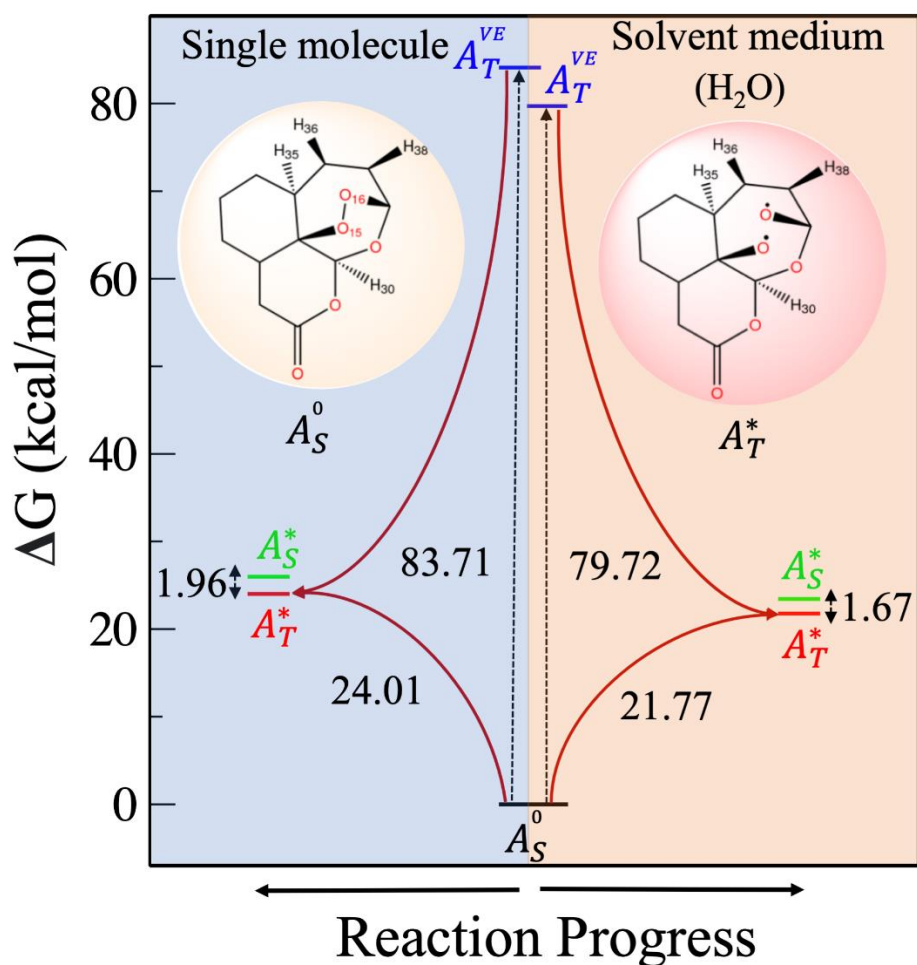


**Fig.3** The diagram depicts the free energy associated with biradical activation in a single molecule environment (left panel) and water medium (right panel). The vertical singlet-triplet free energy gap of 83.71 kcal/mol computed at the neutral singlet state geometry in single molecule environment, while in the water medium it is 79.72 kcal/mol. The free energy difference between the neutral artemisinin and the activated one ( $A_T^*$ ) is 24.01 kcal/mol in gas-phase and 21.77 in water medium. In the following section the detailed energetic perspectives of the various biradical intermediates are provided through which the propagations of chemical reactions occur.

### 3.2. Chemical rearrangements of the activated *Bi-radical* and reaction propagations

The activation of artemisinin generates the oxygen-centered bi-radical that is highly unstable and reactive. This is why the generated O-centered radical immediately undergoes various H-shift chemical rearrangement reactions<sup>57-58</sup> through quantum tunneling of the hydrogen atoms and produces thermodynamically more stable biradical intermediates.

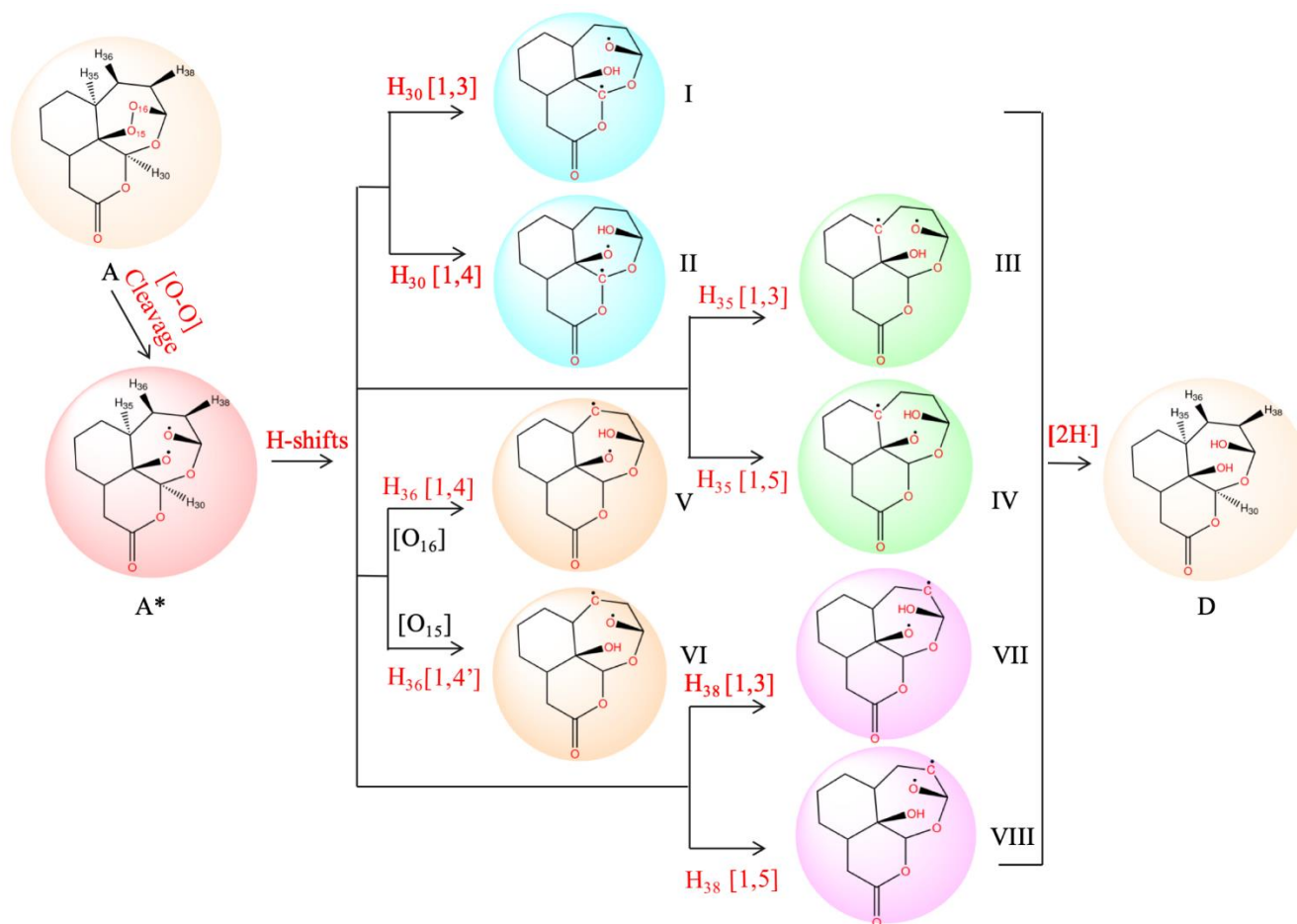


**Fig.4** I to VIII are the possible different biradical intermediate species that could be generated by homolytic cleavage of O-O bond in artemisinin followed by H-shift rearrangements. The resulting H-shift rearrangements are depicted as H<sub>x</sub> [n, m], where x is the serial no of H-atom as shown in Fig. 1a. For example, H<sub>30</sub> [1,3] hydrogen shift indicates the H-atom with the atomic index 30 migrates to a new position two atoms away (i.e., 1, 3 shift) from its original position.

Taking the advantage of CDFT to precisely localize the radical centers within the specific atomic sites, we have investigated the lowest energy H-shifted rearranged biradicals through which further chemical reactions are likely to occur. It is hypothesized that the energetically more stable rearranged biradicals are predominantly formed and route the propagation of the chemical reaction through the thermodynamically stable biradical intermediates.

All the possible hybrid biradical intermediates (I to VIII, Fig. 4) upon the hydrogen shift rearrangements are explicitly investigated in this study. The intramolecular H-shift is quite common but a quantum mechanical phenomenon. The probability of occurrence for the thermodynamically stable species via the quantum chemical rearrangement route is more probable in terms of chemical reaction dynamics perspectives. The computed differences of free energies ( $\Delta G$ ) of the intermediate diradicals along with neutral artemisinin with respect to the activated bi-radical (triplet) state are plotted in concise form in Fig. 5 and  $\Delta E$ ,  $\Delta H$  along

with the entropic contributions are provided in Table 1. The dominant contribution to  $\Delta G$  and  $\Delta H$  mainly arises from the  $\Delta E$ . A very small contribution of  $\Delta S$ , which is almost similar for all the different intermediates, has also been noticed.

**Table 1.** Computed *Ab-initio* thermodynamic parameter for artemisinin where  $\Delta E$  is the change in electronic Energy,  $\Delta G_{298.15K}$  is Gibbs free-energy change,  $\Delta H$  is the enthalpy change and  $\Delta S$  is the entropy change. All these quantities are provided in kcal/mol.

Routes	$\Delta E$	$\Delta G_{298.15K}$	$\Delta H_{298.15K}$	$\Delta S$
$A_S^0 \rightarrow A_{T}^{VE}$	84.11	83.71	83.71	0.0015
$A_S^0 \rightarrow A_T^*$	25.00	24.01	24.03	0.0036
$A_T^* \rightarrow A_S^*$	1.87	1.96	1.96	-0.0002
$A_T^* \rightarrow I$	-9.66	-9.80	-9.79	0.0041
$A_T^* \rightarrow II$	-8.32	-8.16	-8.47	0.0039
$A_T^* \rightarrow III$	1.29	0.98	0.98	0.0052
$A_T^* \rightarrow IV$	-3.72	-3.10	-3.09	0.0064
$A_T^* \rightarrow V$	-6.33	-7.04	-6.04	0.0009
$A_T^* \rightarrow VI$	-0.71	-1.37	-0.37	0.0085
$A_T^* \rightarrow VII$	-2.06	-2.25	-2.24	0.0094
$A_T^* \rightarrow VIII$	2.58	0.58	0.58	0.0033

In Fig.5, the free energy differences plotted for the activated biradical ( $A_T^*$ ) to all the possible rearranged hybrid intermediate species. Finally, the H-atom addition reaction to form diol from those rearranged intermediates are also provided. It has been observed that among the eight biradical intermediates, two intermediates i.e., III and VIII that have been formed from  $H_{35}$  [1,3] and  $H_{38}$  [1,5] shifts with  $\Delta G$  values of +0.98 and +0.58 kcal/mol are thermodynamically quite unfavorable. While the other six biradical intermediates are having  $\Delta G$  negative values indicating thermodynamically favorable species. Out of the six stable intermediates, we realized that only I and II i.e., product of the  $H_{30}$  [1,3] and  $H_{30}$  [1,4] rearrangement reactions, are most stable (See Fig. 4 & Table 1) with  $\Delta G$  values of -9.80 and -8.16 kcal/mol respectively. These carbon centered radicals (I & II) are most stable because the radical center in both the cases are surrounded by the two O-atoms that allows a significant amount of spin-density to be delocalized from the radical site to itself. This provided the stability to these radicals. However, such conditions are not prevailed in the other cases as radical centers are mostly surrounded by the  $sp^3$  C-atoms and thus does not provide the stability due spin-density de-localization.<sup>59</sup> It is

thus predicted that the propagation of chemical reactions are most likely to occur through the intermediate I and II along with the mixing with the other intermediates to some extent.

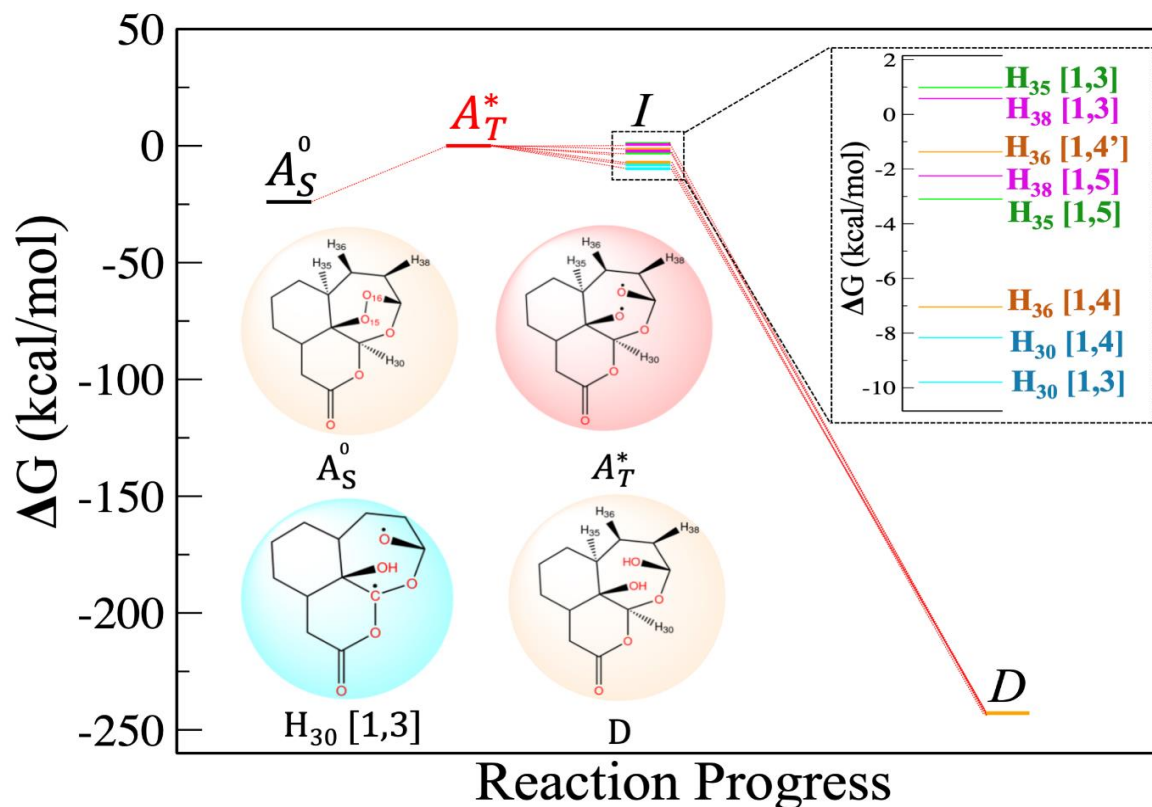


**Fig. 5** The diagram depicts the free energy change in neutral and activated *bi-radical* intermediates through which chemical reaction occurs. Out of all the H-shift rearrangements  $H_{30}$  [1,3] is a more stable biradical-intermediate.

#### 4. Conclusions & Outlook

The free energy of activation ( $\Delta G$ ) of artemisinin associated for the homolytic cleavage is lesser (+21.77 kcal/mol) than the heterolytic cleavage (+23.64 kcal/mol). This suggests that the activation of artemisinin is quite viable even without any transfer of electrons. The spontaneous homolytic cleavage of the O-O bond upon singlet to triplet excitation of the neutral artemisinin also indicates the involvement of the bi-radical intermediates in the mechanistic aspect of anti-malarial activities. It is observed that a few hybrid bi-radical intermediates formed upon intramolecular hydrogen-shift rearrangements are thermodynamically quite stable compared to oxygen-centered biradical. The hybrid-biradical intermediate I & II are found to be the most favorable bi-radical intermediate upon [1,3] and [1,4] H-shift (i.e.,  $H_{30}$  [1,3] and  $H_{30}$  [1,4]) by -9.80 and -8.16 kcal/mol respectively. These intermediate bi-radicals are quite stable than the

activated artemisinin by -9.80 kcal/mol and expected to play the dominant role in the reaction mechanism propagation in the antimalarial activities.

The homolytic cleavage of the endoperoxide bonds has been realized in various theoretical as well as experimental perspectives but in different endoperoxide complexes. However, its association with the artemisinin's mechanism of action for the anti-malarial drug is yet to be established in the literature through dedicated studies. Till date, most of the mechanistic studies have been performed with the notion of monoradical perspectives only which seems to be energetically not true. Thus, further dedicated and sophisticated mechanistic studies are required to understand the complete mechanism. The experimental realization of the studied objectives might inculcate a twist in the tail as the currently accepted activation of artemisinin through the reductive mono-radical pathways only. The trigger for homolytic cleavage of the endoperoxide bonds at the food vacuole of the malaria parasites is another domain to be established and we are further working on the mechano-chemical aspect of homolytic cleavage. We are further anticipating that such triggers for the homo-lytic cleavage at non-parasite locations may lead to the inefficacy of the artemisinin that might be correlated with growing drug resistance.

### **Associated Content**

#### **Supporting Information**

Gibbs-free energy calculations, Lowdin spin-density analysis, Computed Total energies and free energy in solvent medium.

### **Acknowledgements**

The authors thank Prof. Peter M. Oppeneer for various helpful discussions and acknowledge the financial support from the Department of Science and Technology through SERB-ECR project no. ECR/2016/000362 and Indo-Sweden joint project no. DST/INT/SWD/VR/P-01/2016. The Ph.D. fellowship support by the Institute of Nano Science and Technology (INST) is highly acknowledged.

### **Conflicts of interest**

There are no conflicts of interest to declare.

### **References**

1. R. W. Snow, C. A. Guerra, A. M. Noor, H. Y. Myint and S. I. Hay, *Nature* 2005, **434**, 214-217.
2. J. Saches and P. Malaney, *Nature*, 2002, **415**, 680-685.
3. S. I. Hay, C. A. Guerra, A. J. Tatem, A. M. Noor and R. W. Snow, *Lancet.Infect. Dis.*, 2004, **4**, 327-36.
4. WHO "World Malaria report 2020." <https://www.who.int/publications-details/world-malaria-report-2020/report/en/>.
5. F. Prugnolle, P. Durand, B. Ollomo, L. Duval, F. Ariey, C. Arnathau, J. P. Gonzalez, E. Leroy and F. Renaud, *PLoS Pathog.*, 2011, **7**, 1371.
6. S. E. Francis, D. J. Sullivan JR and D. E. Golgberg , *Annu. Rev. Microbiol.*, 1997, **51**, 97-123.
7. S. Kumar, M. Guha, V. Choubey, P. Maity and U. Bandyopadhyay, *Life Sci.*, 2007, **80**, 813-28.
8. L. M. Coronado, C. T. Nadovich and C. Spadafora, *Biochim. Biophys. Acta.*, 2014, **1840**, 2032-2041.
9. M. E. Ali and P. M. Oppeneer, *Chem. Eur. J.*, 2015, **21**, 8544-8553.
10. R. Thome, S. C. P. Lopes, F.T.M. Costa and L. Verina, *Immunol. Lett*, 2013, **153**,50-7.
11. J. Achan, A. O. Talisuna, A. Erhart, A. Yeka, J. K. Tibenderana, F. N. Baliraine, P. J. Rosenthal and U. D. Alessandro, *Malar J*, 2011, **10**, 144.
12. T. J. Egan, D. C. Ross and P. A. Adams, *FEBS Lett.*, 1994, **352**, 54-7.
13. T. E. Wellems and C.V.Plowe, *J. Infect. Dis.*, 2001, **184**, 770-776.
14. D. L. Klayman, *Science*, 1985, **228**, 1049-55.
15. S. R. Meshnick, T. E. Taylor and S. Kamchonwongpaisan, *Microbiol. Rev.*, 1996, **60**, 301-315.
16. P. M. O'Nil, V. E. Barton and S. A. Ward, *Molecules*, 2010, **15**,1705-1721.
17. S. R. Meshnick, *Int. J. Parasitol.*, 2002, **32**, 1655-1660.
18. S. R. Meshnick, A. Thomas, A. Ranz, C.M. Xu and H. Z. Pan, *Mol. Biochem. Parasitol.*, 1991, **49**, 181-189.
19. J. Q. Araujo, J. W. de Mesquita Carneiro, M .T. de Araujo, F. H. A. Leite and A. G. Taranto, *Bioorg. Med. Chem.*, 16, **2008**. 5021-5029.
20. S. R. Meshnick, Y. Z. Yang, V. Lime, F. Kuypers, S. Kamchonwongpaisan and Y. Yuthavong, *Antimicrob. Agents. Chemother.*, 1993, **37**, 1108-1114.
21. G. H. Posner and C. H. Oh , *J. Am. Chem. Soc.*, 1992, **114**, 8328-8329.

22. W. M. Wu, Y. Wu, Y. L. Wu, Z. J. Yao, C. M. Zhou, Y. Li and F. Shan, *J. Am. Chem. Soc.* 1998, **120**, 3316-3325.
23. P. M. O'Neil, L. P. D. Bishop, N. L. Searle, J. L. Maggs, R. C. Storr, S. A. Ward, B. K. Park and F. Mabbs, *J. Org. Chem.* 2000, **65**, 1578-1582.
24. S. Zhang and G. S. Gerhard, *Bioorg. Med. Chem.*, 2008, **16**, 7853-7861.
25. J. Wang, C. J. Zhang, W. N. Chia, C. C. Y. Loh, Z. Li, Y. M. Lee, Y. He, L. X. Yuan, T. K. Lim, M. Liu, C. X. Liew, Y. Q. Lee, J. Zhang, N. Lu, C. T. Lim, Z. C. Hua, B. Liu, H. M. Shen, K. S. W. Tan and Q. Lin, *Nature*, 2015, **6**, 10111.
26. S. Zhang and G. S. Gerhard, *Bioorg. Med. Chem.*, 2008, **16**, 7853-7861.
27. G. H. Posner, D. Wang, J. N. Cumming, C. H. Oh, A. N. French, A. L. Bodley and T. A. Shapiro, *J. Med. Chem.*, 1995, **38**, 2273-2275.
28. M. S. C. Pereira, R. Kiralj, M. M. C. Ferreira, *J. Chem. Inf. Model*, 2008, **48**, 85-98.
29. J. Gu, K. Chen, H. Jiang and J. Leszczynski, *J. Phys. Chem. A* , 1999, **103**, 9364-9369.
30. M. G. B. Drew, J. Metcalfe and F. M. D. Ismail, *J. Mol. Struct.*, 2004, **711**, 95-105.
31. A. G. Taranto, J. W. de Mesquita Carneiro and M. T. de Araujo, *Bioorg. Med. Chem.*, 2006, **14**, 1546-57.
32. P. Moles, M. Oliva and V. S. Safont, *Tetrahedron*, 2008, **64**, 9448-9463.
33. J. Gu, K. Chen, H. Jiang and J. Leszczynski, *J. Mol. Struct.*, 1999, **491**, 57-66.
34. A. G. Taranto, J. W. de M. Carneiro and F. G. Oliveira, *J. Mol. Struct.*, 2001, **539**, 267-272.
35. C. L. Dufaure, F. Najjar and C. A. Barres, *J. Mol. Struct.*, 2007, **803**, 17-21.
36. A. J. Lin, D. L. Klayman and J. M. Hoch, *J. Org. Chem.*, 1985, **50**, 4504-4508.
37. S. Tonmunpheap, S. Irle, S. Kokpol, V. Parasuk and P. Wolschann, *J. Mol. Struct.*, 1998, **454**, 87-90.
38. E. M. Bras, L. I. L. Cabraal, P. S. M. Amado, M. Abe, R. Fausto and M. L. S. Cristiano, *J. Phys. Chem. A.*, 2020, **124**, 4202-4210.
39. C. A. Barres, Y. Carissan and B. Tuccio, *ACS Omega.*, **2017**, **2**, 5357-5363.
40. F. Najjar, C. A. Barres, R. Lauricella, L. Gorrichon and B. Tuccio, *Tetrahedron Lett.* 2005, **45**, 2117-2119.
41. B. Kaduk, T. Kowalczyk and T. V. Voorhis, *Chem. Rev.*, 2012, **112**, 321-370.
42. M. E. Ali, N. N. Nair, V. Staemmler and D. Marx, *J. Chem. Phys.*, 2012, **136**, 22410.
43. Q. Wu and T. V. Voorhis, *J. Phys. Chem. A.*, 2006, **110**, 9212-9218.
44. A. D. Becke, *J. Chem. Phys.*, 1993, **98**, 5658-5652.
45. J. T. Rives and W. L. Jorgensen, *J. Chem. Theory. Comput.*, 2008, **4**, 297-306.

46. F. Neese, Wiley Interdiscip. Rev.: Comput., Mol. Sci. 2012, **2**, 73–78.
47. M. Valiev, E. J. Bylaska, N. Govind, K. Kowalski, T. P. Straatsma, H. J. J. Van Dam, D. Wang, J. Nieplocha, E. Apra, T. L. Windus and W. A. de Jong, Comput. Phys. Commun., 2010, **181**, 1477–1489.
48. Z. Zhao, P. Bai, L. Li, J. Li, L. Wu, P. Huo and L. Tan, *Materials*, 2019, **12**, 330.
49. A. Govender, D. C. Ferre and J.W. Niemantsverdriet, *Chem. Phys. Chem.*, 2012, **13**, 1591-1596.
50. G. F. Bauerfeldt, G. Arbilla and E. C. da Silva, *J. Braz. Chem. Soc.*, 2005, **16**, 190-196.
51. A. A. Voityuk and S. F. Vyboishchikov, *Phys. Chem. Chem. Phys.*, 2019, **21**, 18706-18713.
52. A. A. Lapkin, M. Peters, L. Greiner, S. Chemat, K. Leonhard, M. A. Liauw and W. Leitner, *Green Chem.*, 2010, **12**, 241-251.
53. R. A. Marcus, *Rev. Mod. Phys.*, 1993, **65**, 599-610.
54. R. B. Yelle and T. Ichiye, *J. Phys Chem. B.*, 1997, **101**, 4127-4135.
55. J. A. Gamez, L. S. Andres and M. Yanez, *Phys. Chem. Chem. Phys.*, 2010, **12**, 1042-
56. X. Zeng, H. Hu, X. Hu, A. J. Cohen and W. Yang, *J. Chem. Phys.*, 2008, **128**, 124510.
57. E. Praske, R. V. Otkjaer, J. D. Crouse, J. C. Hethcox, B. M. Stoltz, H. G. Kjaergaard and P. O. Wennberg, *J. Phys. Chem. A.*, 2019, **123**, 590-600.
58. M. M. Savitski, F. Kjeldsen, M. L. Nielsen and R. A. Zubarev, *J. Am. Soc. Mass Spectrom*, 2007,**18**, 113-120.
59. A. Bajaj and M.E. Ali, *J. Phys. Chem. C.*, 2019, **123**, 15186-15294.